Orientational phase transition in monolayers of multipolar straight rigid rods: The case of 2-thiophene molecule adsorption on the Au(111) surface

G. dos Santos *
Facultad de Ingeniería, Universidad de Mendoza, CONICET Mendoza, Argentina and Departamento de Física, Instituto de Física Aplicada, Universidad Nacional de San Luis-CONICET, D5700HHW San Luis, Argentina

E. Cisternas
Departamento de Ciencias Físicas, Universidad de La Frontera, Casilla 54-D, Temuco, Chile

E. E. Vogel
Departamento de Ciencias Físicas, Universidad de La Frontera, Casilla 54-D, Temuco, Chile and Center for the Development of Nanoscience and Nanotechnology (CEDENNA), 9170124 Santiago, Chile

A. J. Ramirez-Pastor
Departamento de Física, Instituto de Física Aplicada, Universidad Nacional de San Luis-CONICET, D5700HHW San Luis, Argentina

(Received 25 August 2022; accepted 9 January 2023; published 25 January 2023)

Monte Carlo simulations and finite-size scaling theory have been carried out to study the critical behavior and universality for the isotropic-nematic (IN) phase transition in a system of straight rigid pentamers adsorbed on a triangular lattice with polarized nonhomogeneous intermolecular interactions. The model was inspired by the deposition of 2-thiophene molecules over the Au(111) surface, which was previously characterized by experimental techniques and density functional theory. A nematic phase, observed experimentally by the formation of a self-assembled monolayer of parallel molecules, is separated from the isotropic state by a continuous transition occurring at a finite density. The precise determination of the critical exponents indicates that the transition belongs to the three-state Potts universality class. The finite-size scaling analysis includes the study of mutability and diversity. These two quantities are derived from information theory and they have not previously been considered as part of the conventional treatment of critical phenomena for the determination of critical exponents. The results obtained here contribute to the understanding of formation processes of self-assembled monolayers, phase transitions, and critical phenomena from novel compression algorithms for studying mutual information in sequences of data.

DOI: 10.1103/PhysRevE.107.014133

I. INTRODUCTION

Molecular self-assembly has emerged in recent years as a useful approach for designing and fabricating new materials [1,2]. In addition, self-assembly has been considered to be central to understanding structure formation in living systems [3]. As a consequence, an increasing interest has been devoted to enhance our understanding of the theoretical basis of the fundamental mechanisms governing self-assembly and the observables required to characterize the interactions driving thermodynamic self-assembly transitions [4–7].

On the other hand, the study of orientational phase transitions in systems of large particles in solution is one of the central problems in statistical mechanics and has been attracting a great deal of interest since long ago. A seminal contribution to this subject was made by Onsager [8], who predicted that very long and thin rods interacting with only excluded-volume interaction can lead to long-range orientational (nematic) order. The nematic phase, characterized by a big domain of parallel molecules, is separated from an isotropic state by a phase transition occurring at a finite critical density. This phase transition is called isotropic-nematic (IN) phase transition.

In two dimensions, the nature of the IN phase transition depends crucially on the particle interactions and a rich variety of behaviors has been observed [9,10]. In the case of lattice-gas models, which is the topic of this paper, a system of straight rigid rods of length k (k-mers) on a square lattice, with two allowed orientations, was studied by Ghosh and Dhar [11]. Using Monte Carlo (MC) simulations and analytical arguments, the authors found strong numerical evidence showing that the system presents nematic order at intermediate densities for $k \geqslant 7$ and provided a qualitative description of a second phase transition (from a nematic order to a nonnematic state) occurring at a density close to 1. This second phase transition was called nematic-isotropic (NI) phase transition. The existence of the nematic phase was analytically demonstrated by Disertorti and Giulani [12]. In addition, the presence of the isotropic-nematic phase transition in a

*gonzalodossantos@gmail.com

particular lattice, called random locally treelike layered lattice, was rigorously demonstrated by Dhar *et al.* [13].

Based on the pioneering work of Ghosh and Dhar [11], a series of papers have been produced pointing to the detailed study of the orientational phase transitions occurring in a system of long straight rigid rods on two-dimensional (2D) lattices with discrete allowed orientations [14–25]. In the case of the first phase transition, it was shown that (1) the universality of the IN transition is consistent with the 2D Ising class for square lattices and the three-state Potts class for honeycomb and triangular lattices [14,15]; (2) the minimum value of k which allows the formation of a nematic phase is $k = 7$ for triangular lattices [16] and $k = 11$ for honeycomb lattices [15]; (3) the orientational order survives in a wide range of lateral interactions between the adsorbed k-mers [17,18]; (4) the critical density characterizing the IN transition θ_1 follows a power law [16,19,20] as $\theta_1(k) \propto k^{-1}$; and (5) an Ising behavior is found for a 2D Zwanzig fluid of hard line segments which may orient either horizontally or vertically [19]. With respect to the second NI phase transition, numerical evidence was provided for the existence of this phenomenon [21–23].

An alternative numerical method to treat orientational phase transitions was applied to the hard-rod problem on 2D lattices [24,25]. The approach is based on the application of information theory using Shannon entropy and data compressor WLZIP for the recognition of repetitive data in time series such as those generated in MC simulations of magnetic systems [26–28]. In addition, new order parameters were defined, which allow a better characterization of the phases occurring in the system.

Very recently, the problem of straight rigid rods of length k adsorbed on square lattices has been investigated in the high coverage regime [29–31]. In Ref. [29], Dhar and Rajesh showed that, in the limit of large k, the configurational entropy per site of fully covered lattices tends to $k^{-2} \ln k$. This theoretical finding was confirmed numerically using MC simulations in the grand-canonical ensemble and thermodynamic integration method [30]. The nature of the NI transition has been addressed in Ref. [31]. Based on perturbation theory, the authors found that, for large k, the second phase transition is a first-order transition with a discontinuity in density in all dimensions greater than 1.

Orientational phase transitions have also been observed in monolayers of strongly anisotropic particles. Such "patchy" particles offer the possibility to be used as building blocks of specifically designed self-assembled structures. In this line, an interesting model was introduced by Tavares *et al.* [32], where effectively attractive patches induce the reversible self-assembly of particles into chains. The system consists of monomers with two attractive (sticky) poles that polymerize reversibly into polydisperse chains and, at the same time, undergo a continuous isotropic-nematic (IN) phase transition. Using an approach in the spirit of the Zwanzig model [33], the complete coverage-temperature phase diagram of the system was obtained. The authors assumed that the IN phase transition for the polydisperse 2D Zwanzig model remains in the 2D Ising universality class.

From the work by Tavares *et al.* [32], several papers exploring the self-assembled rigid rods (SARRs) model have been published [34–40]. These studies confirmed that, in the case of square lattices, the universality class of the SARRs model is in the 2D Ising class, as in models of monodisperse rigid rods [14,15]. A similar scheme was observed for triangular lattices, where grand-canonical MC simulations indicated that the IN transition of SARRs at intermediate density belongs to the $q = 3$ Potts-type universality class. The same universality class had been reported for monodisperse rigid k-mers on triangular lattices [14,15].

In the papers mentioned so far, the studied models correspond to highly idealized systems. The cost of introducing these precursor models is the lack of some experimental features presented by real systems. However, the obtained results have been very useful as a help and a guide to establish a general framework for the study of this kind of systems. In this sense, one of the most important conclusions of this task is that the interplay between the self-assembly process and the nematic ordering is a distinctive characteristic of these systems. This finding stimulates the development of more sophisticated models which can be able to reproduce concrete experimental situations.

In this context, we focus in the present paper on a system of 2-thiophene curcuminoid molecules adsorbed on the Au(111) surface. In a recent paper from our group [41], this system was modeled using a lattice-gas of linear pentamers adsorbed onto a triangular lattice. The model includes intermolecular multipolar interactions between neighboring pentamers, and it was able to reproduce the interaction energies of the most representative orientations of the 2-thiophene molecules over the Au surface which were obtained from previous DFT calculations [42]. By simulating the deposition process under a MC scheme, an IN phase transition was identified, indicating the formation of a self-assembled monolayer, reproducing the experimental observations [42,43].

The lattice-gas model of interacting pentamers represents an advance over previous work [32–40] in two main ways. First, the adsorbate is a molecule formed by five units, each occupying one adsorption site on the surface. Most adsorbates involved in experiments, except noble gases, are polyatomic; hence, the theoretical description of their thermodynamic properties is a topic of much interest in adsorption theory. This subject is generically called multisite-occupancy adsorption, and it has been referred to as the prototype of the lattice problem [44]. In Refs. [32–40], it is supposed that each adsorbed molecule has spherical symmetry and occupies one lattice site. In the limit of zero lateral interactions (infinite temperature), the arrangement of the adsorption sites in space is immaterial, and consequently, the single-occupancy model does not distinguish between different lattice geometries. The same does not happen with the multisite-occupancy scheme presented here, where the thermodynamic properties of the adlayer are significantly affected by the spatial correlations between adsorption sites, even for molecules that do not interact laterally. Second, the pentamers are considered to have three interaction centers, both ends (heads), and the central segment. The heads are of the same kind, while the segment at the center is of a different kind. Such distribution leads to three different basic interactions (head-head, head-center, and center-center) and is capable to capture the high-polarity nature of these 2-thiophene curcuminoid molecules. The

numerical values of the interaction energies are set according to DFT calculations performed by Flores *et al.* [42]. In the case of Refs. [32–40], the lateral interaction scheme is very simple: monomers with two attractive poles.

Despite these recent results there are remaining questions to be answered: "What type of phase transition is it?," "What is its nature?," "Does it belong to a known universality class?" The objective of this paper is to provide a thorough study in this direction. For this purpose, extensive MC simulations supplemented by analysis using finite-size scaling (FSS) theory [45–49] have been carried out to study the critical behavior of the system introduced in Ref. [41]: interacting linear pentamers adsorbed on triangular lattices. A nematic phase, characterized by a big domain of parallel pentamers, is separated from the disordered state by a continuous phase transition occurring at a finite critical lattice coverage (or density). Based on the strong axial anisotropy of the nematic phase, an order parameter measuring the orientation of the particles has been introduced. Taking advantage of its definition, we were able to study for the first time the universality class of the IN phase transition occurring in the system. The accurate determination of the critical exponents revealed that the IN transition belongs to the 2D three-state Potts universality class.

The study was complemented by an alternative numerical method to treat phase transitions. The approach is based on the use of information theory using data compression techniques, and it has already been successfully used to recognize thermodynamic phases [24–28,50], volatility and critical periods in stock markets [51] and pension funds [52], vascular risk [53], and earthquake risk [54]. In the present paper, quantities derived from data compression algorithms will be used to characterize the IN phase transition occurring at intermediate densities. In particular, these quantities will be employed for the first time for the determination of the critical exponents under the conventional FSS treatment.

This paper is organized as follows. The lattice-gas model and the simulation scheme are described in Secs. II A and II B, respectively. In Sec. II C, the method of data compression to obtain the critical densities is presented. Section III is devoted to the main results of the application of our technique and the comparison with previous results. A summary and general conclusions are given in Sec. IV.

II. MODEL AND METHODS

A. Molecular deposition and lattice-gas model

The adsorption process of 2-thiophene molecules over the Au(111) surface is studied trough a simplified lattice-gas model. In this sense, the gold surface is discretized and modeled as a 2D rhombus-shaped triangular lattice consisting of $M = L \times L$ adsorptive lattice sites, where L is the linear dimension of the lattice. Periodic boundary conditions are considered over the three directions of the lattice.

The 2-thiophene curcuminoids are elongated molecules having two sulfur atoms at each end of a carbon chain. Several hydrogen atoms are distributed along the molecule, while two separate oxygen atoms are located toward the middle, equidistant from the center, see Fig. 1(a). According to previous DFT studies [42], the sulfur atoms are responsible for a strong adsorption energy (5.98 eV) as well for three equivalent preferred directions of the molecules adsorbed in a flat manner onto the Au(111) surface. Furthermore, once the curcuminoid molecules are adsorbed onto the gold surface they experience a charge redistribution. Such charge redistribution explains the electrical multipole appearing on each molecule, which is responsible for the different repulsive interaction intensities depending on the segments of one molecule facing the segments of a neighboring molecule. For details of the molecular structure and its electric charge distribution, see Fig. 1 in Ref. [41].

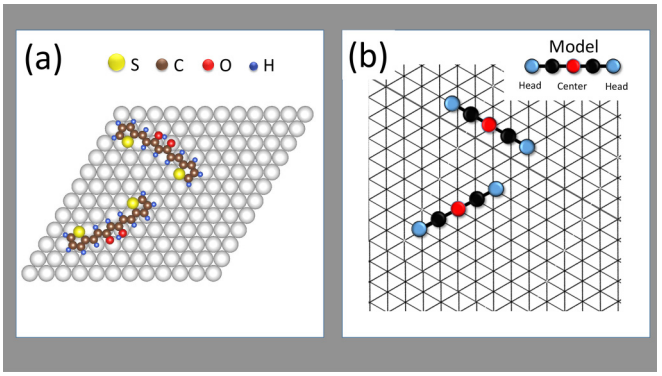

FIG. 1. (a) Simplified schematic diagram showing two curcuminoid molecules adsorbed on the gold surface. (b) Lattice-gas representation of the situation in part (a). The FCC(111) surface is represented by a triangular lattice and the 2-thiophene molecules are modeled as pentamers. Inset: For each 2-thiophene molecule (pentamer), three interaction centers are considered: two at the ends and one at the center.

Based on these aspects, the 2-thiophene molecules are modeled as rigid linear k-mers, with $k = 5$. A linear k-mer is an entity that will adsorb onto the lattice occupying exactly k consecutive lattice sites, consequently we can speak of pentamer adsorption in this case. In addition, when deposited onto the lattice, the pentamers will interact with their nearest neighbors (NN) in several different geometric configurations. We develop here a simple model retaining the most important aspects of these interactions.

Let us first consider proximity: We restrict to interactions of pairs that are NN only. We then consider internal structure and orientation. In order to capture the multipolar essence of these molecules and their intermolecular interactions, three different centers along the pentamers are defined, both ends (heads) and the center element of the chain. The remaining two intermediate elements of the chain are considered neutral, see Fig. 1(b). In this way, the terminal monomers of the chain (heads) will interact differently with the heads than with the central element of another NN pentamer. Therefore, three different interaction energies are defined: head-head (w_{HH}), head-center (w_{HC}), and center-center (w_{CC}).

Generally speaking, the carbon backbone of the molecule tends to be positively charged while the outside is mostly negative. This makes all proximity interaction energies as repulsive or positive. In a simplified way we propose that these interaction energies conveniently expressed in k_BT (k_B is the Boltzmann constant) units, are $w_{\mathrm{HH}} = 1.0$, $w_{\mathrm{HC}} = 0.5 w_{\mathrm{HH}} =$

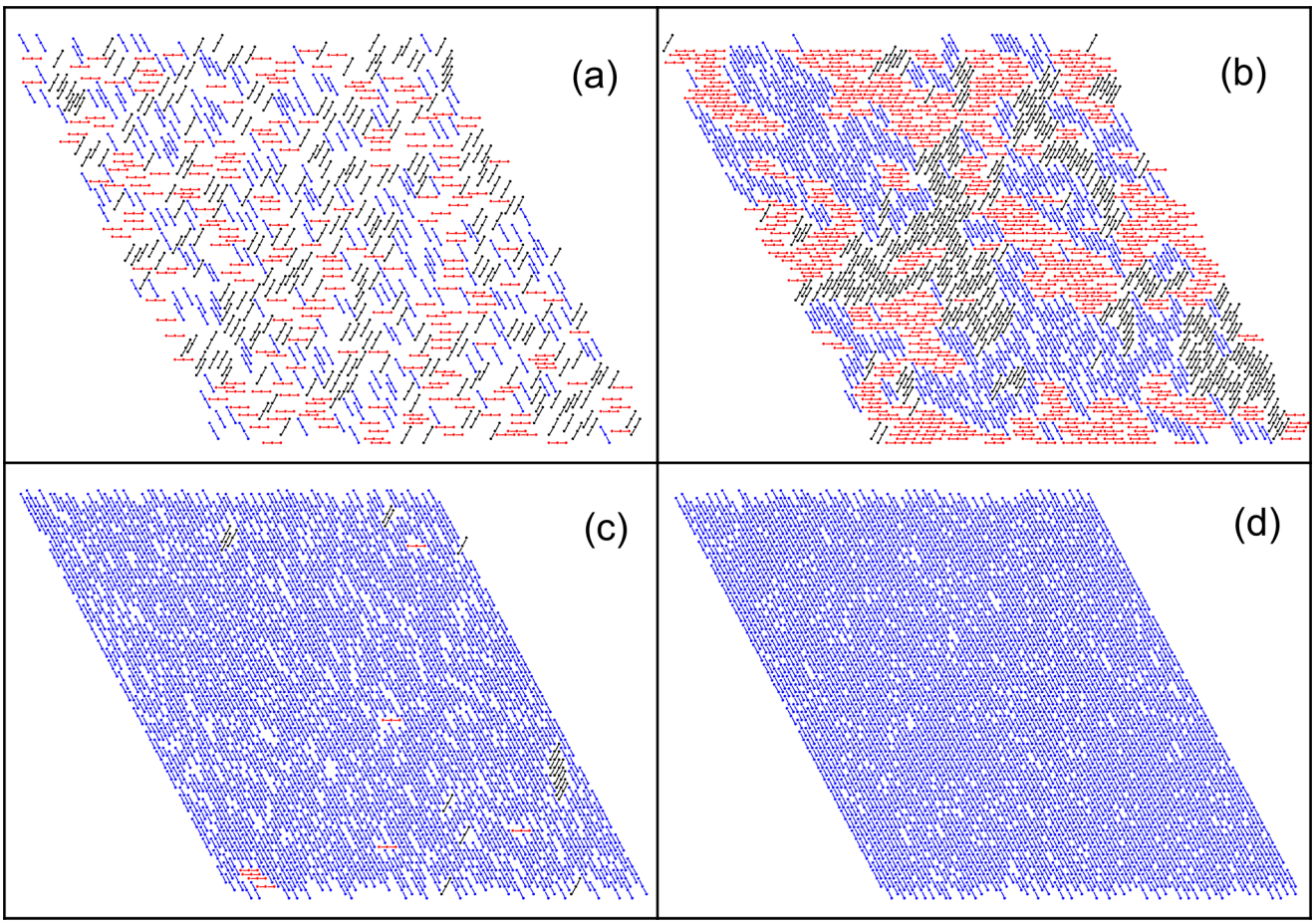

FIG. 2. 4 snapshots of the simulation in order of increasing coverage: (a) $\theta \ll \theta_c$, (b) θ just under θ_c, (c) θ just over θ_c, and (d) $\theta \gg \theta_c$. The polar pentamers are sketched as rods of three segments, representing the two heads and the center element and are colored according to their orientation.

0.5, and $w_{CC} = 1.5 w_{HH} = 1.5$. As explained in our previous paper [41] (see for example Fig. 2 of that paper and the discussion around it), this set of values manages to reproduce very well the interaction energies of two adsorbed 2-thiophene molecules on its most representative relative orientations, as calculated by Flores *et al.* [42] by DFT calculations.

To summarize, our model consist of a 2D rhombus-shaped triangular lattice of adsorption sites in contact with a gas of interacting k-mers with $k = 5$, more specifically polar pentamers. The distance between adjacent segments of a pentamer is equal to the lattice constant a. Under this framework we will consider reversible monolayer adsorption, meaning that the pentamers will adsorb and desorb from the lattice until equilibrium is reached, and a lattice site can host only one segment of a molecule. In addition, the linear pentamers are adsorbed or desorbed without considering any dissociation, reorganization, distortion, or self-diffusion.

The Hamiltonian of this system can be written defining an occupation variable c_i for each lattice site. In this way, $c_i = 0$ if adsorption site i is empty and $c_i = 1$ if it is hosting a segment of a molecule,

$$H = \sum_{\langle i,j \rangle} w_{ij} c_i c_j - \mu N + \varepsilon_0 \sum_{i=0}^{M} c_i. \tag{1}$$

The summation of the first term runs over all nearest-neighbor sites ($\langle i, j \rangle$) and w_{ij} is the interaction energy that may take the values $w_{ij} = w_{HH}, w_{HC}, w_{CC}$ depending on the nature of the monomers adsorbed on the corresponding pair of NN sites as defined above. N is the total number of adsorbed molecules. Finally, the last term represents the adsorption energy of the system, with ε_0 being the adsorption energy of each lattice site. When homogeneous lattices are considered, as is the case of this work, the last term can be dropped without loss of generality.

B. Monte Carlo simulations

The system was studied by means of grand-canonical MC simulations. In this statistical ensemble the free parameters to be set and varied are the chemical potential μ and the interaction energies w_{HH}, w_{HC}, and w_{CC}. We have implemented a typical particle-vacancy adsorption-desorption algorithm according to the Metropolis scheme [55]. Instead of varying the chemical potential sequentially, we have implemented a parallel tempering algorithm [56–58]. Under this framework, several replicas of the system (N_{rep}) are simulated in parallel, each replica having a different value of chemical potential μ between some extreme values μ_0 and μ_f. The difference in chemical potential between adjacent replicas is given simply

by $\Delta\mu = (\mu_f - \mu_0)/N_{\rm rep}$; equivalently, two replicas are considered adjacent if their difference in chemical potential is equal to $\Delta\mu$. The key aspect of this algorithm is that after a fixed number of simulation iterations the configurations of two adjacent replicas are swapped with certain probability. As it will be detailed below, this swapping probability depends on the difference of the total number of adsorbed molecules N and the chemical potential μ between the two replicas to be swapped. This procedure increases the efficiency of the simulations, allowing us to reduce considerably the equilibrium and calculation times, being particularly efficient in unblocking frozen states where the system is occasionally trapped in local energy minimums. The number of replicas in this algorithm is typically chosen such that it generates an exchange probability between adjacent replicas greater than (or on the order of) 50%. In our case we choose $N_{\rm rep} = 100$.

The degree of order in the adsorbed monolayer is calculated introducing an orientational order parameter δ,

$$\delta = \frac{|N_1\vec{v}_1 + N_2\vec{v}_2 + N_3\vec{v}_3|}{N_1 + N_2 + N_3}. \tag{2}$$

Each vector $\vec{v}_i$ is a unitary vector associated to one of the three equivalent directions of the triangular lattice (the three possible orientations for an adsorbed molecule on the lattice) and N_i is the number of adsorbed molecules in the direction i, $i = 1, 2, 3$. In this way, δ varies from 0 (isotropic) to 1 (nematic). In the former, about $1/3$ of the molecules are adsorbed along each of the three directions ($N_1 \approx N_2 \approx N_3 \approx N/3$), so the vector sum nearly vanishes and $\delta \approx 0$. In the nematic case all the N k-mers of the monolayer are nearly aligned along one (any) of the three independent directions leading to $\delta \approx 1.0$.

In what follows some details of the algorithm are given:

(1) Set the values for μ_0 and μ_f and generate $N_{\rm rep} = 100$ replicas of the system.

(2) A random initial configuration is generated in each replica.

(3) One of the $N_{\rm rep}$ replicas is randomly selected.

(4) A set of k (with $k = 5$) consecutive lattice sites (linear k-uple) is sorted. If the k sites of the selected linear k-uple are empty, then an attempt is made to adsorb a pentamer with probability $P = \min\{1, \exp(-\Delta H/k_BT)\}$, where ΔH represents the difference between the Hamiltonians of the final and initial states. If, on the other hand, the k sites of the linear k-uple are occupied by units of the same k-mer (pentamer), an attempt is made to desorb this k-mer with the same probability P; otherwise, the attempt is rejected.

(5) After $M = L \times L$ adsorption or desorption attempts [by following the procedure described in point (4)], the configurations of two adjacent replicas of the system are swapped with probablity $P_{\rm exc} = \min\{1, \exp(-\Delta N\Delta\mu)\}$, where ΔN and $\Delta\mu$ represent the difference in the number of adsorbed molecules and the difference in chemical potential, respectively, between the two replicas to be swapped.

(6) A MC step (MCs) is completed after we repeat (3)–(5) $N_{\rm rep}$ times.

It was found that stable equilibrium states where reached after 5×10^6 MCs. The simulations were run with $r = 10 \times 10^6$ MCs, employing the first $r/2$ MCs to equilibrate the system and the remaining $r/2$ MCs were used to compute the averages of the observables of interest. The effect of finite size was investigated by examining lattices with $L = 50, 75, 100$, and 125, with an effort reaching almost the limits of our computational capabilities.

The surface coverage (or density) θ is monitored for each μ value and its corresponding equilibrium value is calculated as a simple average:

$$\theta = \frac{1}{M}\sum_i^M \langle c_i\rangle, \tag{3}$$

where $\langle ...\rangle$ means time average over the last $r/2$ MCs of the MC simulation.

A similar treatment was done for the order parameter δ. The complete time series for both θ and δ were stored for each value of the chemical potential to be later used by the information theory methods described in next subsection.

In addition, the fourth-order Binder cumulant U_L [49] and the susceptibility χ of the order parameter δ were calculated as

$$\chi = \frac{L^2}{k_BT}[\langle\delta^2\rangle - \langle\delta\rangle^2], \tag{4}$$

and

$$U_L = 1 - \frac{\langle\delta^4\rangle}{3\langle\delta^2\rangle^2}. \tag{5}$$

C. Information recognizer

In the present paper, we apply the data compressor WLZIP [26–28] to the recognition of information content within the dynamical series generated by previous MC simulations. The data recognizer WLZIP was created to find repeated meaningful information in any sequence of data. The recognition of meaningful repetitions is not the same under different circumstances. Near a critical point, where a chaotic succession of data should occur, repetitions of numerical values corresponding to critical functions (such as the order parameter δ) will be seldom and WLZIP will compress very little. Thus, what WLZIP should give is high contrast between monotonic regimes as compared to chaotic regimes. Consequently, each maximum in the quantities derived from the compression process should be indicative of the existence of a critical point. As it will be shown in the next section, this feature is very useful for identifying and characterizing orientational phase transitions in systems of adsorbed large molecules. In the next paragraphs we briefly summarize the way this data recognizer operates.

WLZIP applies to any parameter q stored in a vector file with σ registers. A precision in the number of digits to be recognized is defined and it can be tuned to better recognize the information according to the kind of data under consideration. The sequence is swept along all the σ values. Each different value q_i is stored at the beginning of a row in a new vector file. Each time an already recognized value appears within the sequence the information of the location of this value along the sequence is stored to the right on the row corresponding to this value. So the new file is a map of the original one and no information is lost.

At the end we have a histogram providing two important parameters: (a) the number ℓ^* of rows (different values in the

sequence) and (b) the weight in bytes w^* of the compressed file created in this way. The mutability ζ for the σ values of this parameter q, namely

$$\zeta_{q(\sigma)} = \frac{w^*}{w}, \tag{6}$$

where w is the weight in bytes of the original sequence of σ values of q after equilibrium.

In addition, given the total number of different q_i values (number of rows ℓ^* in the compressed file) over the number of rows in the original file, namely ℓ, defines the diversity $D_{q(\sigma)}$ of the sequence of σ values for the variable q at equilibrium for the chemical potential μ:

$$D_{q(\sigma)} = \frac{\ell^*}{\ell}. \tag{7}$$

We make use of the same information content obtained from the MC time series depicted in the preceding section (along $r = 5 \times 10^6$ MCs). Accordingly, $\sigma = 5 \times 10^6$. For the rest of the paper we will use ζ_q and D_q to denote mutability and diversity, respectively [for simplicity we will drop the "(σ)" label].

III. RESULTS AND DISCUSSION

As mentioned, in our previous paper [41] we found that the system described previously experiences an isotropic-nematic phase transition at a determined critical coverage. Figure 2 shows snapshots of the system experiencing this phase transition. It is clear that nematic order among these repelling k-mers arises over certain critical concentration θ_c. Configurations under θ_c present disorder with no particular tendency to order along any direction. On the other hand, configurations over θ_c present a clear preferred orientation and this property is sustained way over θ_c. If Fig. 2(c) or Fig. 2(d) are compared to the STM image of 2-thiophene molecules adsorbed onto the Au(111) surface as presented in Fig. 2 of Flores *et al.* [42], then the correspondence flows immediately. Thus, our model explains the nematic order that appears in this system. In the rest of the analysis we get deeper into the kind of transition our simulations suggest and the possible dependence of θ_c on other characteristics of the system is established.

Now, we address the study of the critical behavior of the system around this orientational phase transition by means of FSS analysis [45–49]. Our goal is to obtain the critical transition coverage along with different critical quantities such as the critical exponents in order to characterize the nature of the phase transition.

According to FSS theory, the expected behaviors of the order parameter, susceptibility, and fourth-order Binder cumulant at criticality are given by:

$$\delta = L^{-\beta/\nu}\tilde{\delta}(\varepsilon L^{1/\nu}), \tag{8}$$

$$\chi = L^{\gamma/\nu}\tilde{\chi}(\varepsilon L^{1/\nu}), \tag{9}$$

and

$$U_L = \tilde{U}_L(\varepsilon L^{1/\nu}). \tag{10}$$

The last equations are valid for $L \to \infty$ and $\varepsilon \to 0$ in such a way that $\varepsilon L^{1/\nu} =$ finite. In addition, $\tilde{\delta}$, $\tilde{\chi}$, and $\tilde{U}_L$ are scaling

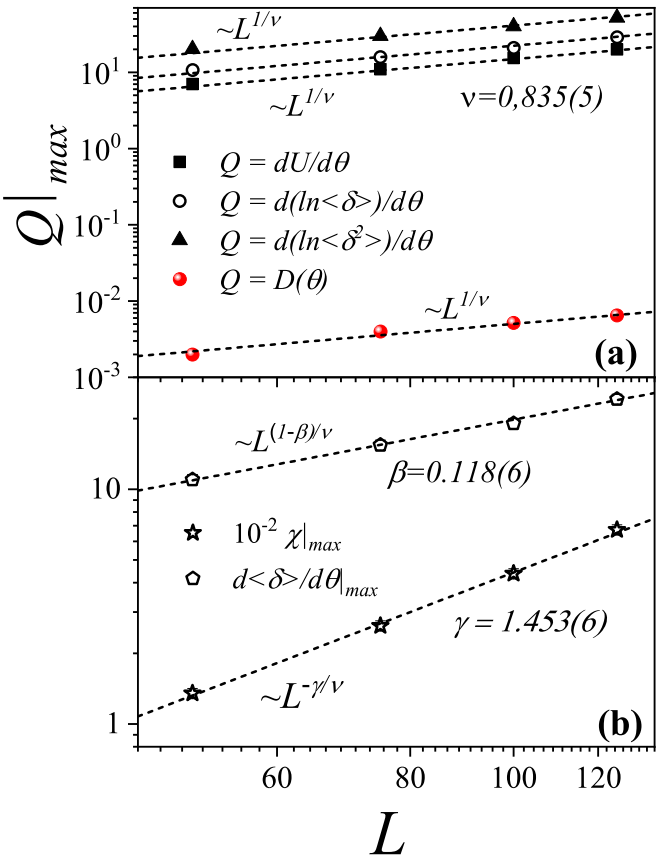

FIG. 3. (a) Log-log plot of the maximum value of the derivative of the Binder cumulant $dU/d\theta$, the logarithmic derivatives of $\langle\delta\rangle$ and $\langle\delta^2\rangle$, and the diversity of the surface coverage $D(\theta)$. Dashed lines represent linear fits proportional to $L^{1/\nu}$. (b) Log-log plot of the maximum value of the derivative of the order parameter $\langle\delta\rangle$ and the maximum of susceptibility χ. Dashed lines represent linear fits proportional to $L^{(1-\beta)/\nu}$ for the maximum value of $\frac{d\langle\delta\rangle}{d\theta}$ and proportional to $L^{-\gamma/\nu}$ for the maximum value of χ.

functions of the respective quantities and β, γ, and ν are the critical exponents related to the order parameter ($\delta \sim -\epsilon^\beta$ for $\epsilon \to 0^-$ and $L \to \infty$), susceptibility ($\chi \sim |\epsilon|^\gamma$ for $\epsilon \to 0$ and $L \to \infty$), and correlation length ($\xi \sim |\epsilon|^{-\nu}$ for $\epsilon \to 0$ and $L \to \infty$), respectively. In the case of conventional FSS theory, $\varepsilon = (T - T_c)/T_c$ is the reduced temperature. In our case, the transition is not temperature driven so ε is defined as the "reduced coverage" $\varepsilon = (\theta - \theta_c)/\theta_c$.

Following Ref. [59], one of the methods for the determination of the critical exponent ν is related with the scaling behavior of the derivatives of certain thermodynamic quantities with respect to density (or coverage) θ. These classical quantities can be, for example, the derivative of the cumulant and the logarithmic derivatives of δ and δ^2. In Fig. 3(a) we have plotted the maximum value of these derivatives as a function of system size in logarithmic scale. As a complementary analysis, the plot includes the scaling behavior of the maximum of the diversity, an indicator that belongs to the information theory and it is not a traditional quantity in the FSS theory. Fitting the first three curves [$dU_L/d\theta$, $d(ln\langle\delta\rangle)/d\theta$ and $d(ln\langle\delta^2\rangle)/d\theta$] we get an estimate of the critical exponent, $\nu = 0.835(5)$. Although the diversity scaling

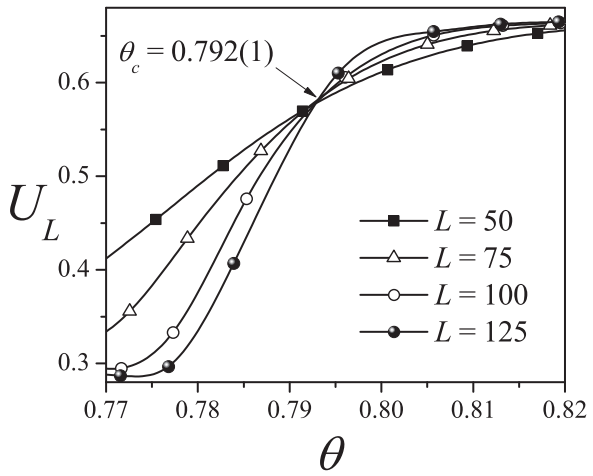

FIG. 4. Fourth-order Binder cumulant $U_L(\theta)$ curves as a function of the lattice coverage θ for different sizes: $L = 50$, solid squares; $L = 75$, open triangles; $L = 100$, open circles; and $L = 125$, spheres. The critical lattice coverage θ_c is obtained from the intersection point of the curves.

behavior was not taken into account for the determination of ν, we can confirm the striking result that this quantity shows similar results than the classical FSS quantities and therefore it might be employed as an alternative quantity to determine the exponent ν.

Having determined ν, the standard procedure to find the critical exponent γ is related to the scaling behavior of the maximum value of the susceptibility, $\chi(\theta)|_{\max}$ [59]. Figure 3(b) shows the result of such scaling along with the estimate for the critical exponent, resulting in $\gamma = 1.453(6)$. The exponent β can now be obtained from the scaling behavior of the maximum value of the derivative of the order parameter, $\frac{d\langle\delta\rangle}{d\theta}|_{\max}$. The results of this scaling are also shown in Fig. 3(b), where the resulting value for the exponent is $\beta = 0.118(6)$.

The obtained values for the critical exponents $\nu \approx 5/6$, $\gamma \approx 13/9$, and $\beta \approx 1/9$ indicate that the transition observed in this system belongs to the $q = 3$ two-dimensional Potts universality class [60]. This finding is consistent with the three competing ordered states near the transition, as reflected by the three components of the corresponding order parameter. A similar behavior has been observed for the simpler case of noninteracting straight rigid rods adsorbed on triangular and honeycomb lattices with three allowed orientations [14,15].

The universality class and scaling behavior of this transition can be further tested from data collapsing techniques following Eqs. (8), (9), and (10). As a first step the critical transition coverage need to be determined. In Fig. 4 we present the fourth-order Binder cumulant curves plotted as a function of θ for the four studied system sizes ($L = 50$, 75, 100, and 125). As it is known, the critical coverage θ_c can be estimated from the intersection point of the curves [49]. Due to small statistical errors and data discreteness, these curves do not all intersect at a single and well-defined point but rather there is a region of intersections. Then, in our case, the critical coverage obtained from the crossing of the cumulants is determined as follows: (1) to improve the accuracy, and using spline fitting, the different curves of U_L are expressed as a function of continuous values of θ and (2) the interval where the curves cross each other is determined. The center of this interval represents the critical point θ_c and the width of the interval is the error in the determination of θ_c. In Fig. 4, this interval is (0.791, 0.793); accordingly, $\theta_c = 0.792(1)$. We have verified that increasing the number of simulation points does not significantly affect the obtained critical coverage.

The existence of a nematic phase in the model proposed here is an interesting result from a theoretical point of view. In fact, as has been reported in a previous work [16], the minimum value of k which allows the formation of a nematic phase is $k = 7$ for a lattice-gas of independent straight rigid k-mers (rods interacting with excluded-volume interactions only) adsorbed on triangular lattices. The effect of nonzero lateral interactions on the critical behavior of this system has not been investigated yet. However, for surfaces with square geometry, it has been found that the presence of homogeneous lateral couplings between the adsorbed k-mers does not modify the value of the critical size k above which the orientational order appears [17,18]. By homogeneous lateral couplings, we refer to the case where the interaction between NN units belonging to different k-mers takes a constant value.

The results obtained in the current study indicate that the critical behavior of adsorbed rigid k-mers is strongly affected by the existence of different interaction centers (nonhomogeneous lateral interactions) in the adsorbate. In the specific case considered here, an isotropic to nematic phase transition is found for $k < 7$, contrary to what was observed for systems with homogeneous (and zero) lateral interactions [17,18]. This issue encourages the investigation of straight rigid k-mers adsorbed on two-dimensional substrates in the presence of nonhomogeneous lateral interactions. A study in this direction is in progress.

With the calculated value for the critical lattice coverage, the critical exponent ν can be obtained from Eq. (10). According to this equation, the curves of U_L vs $\varepsilon L^{1/\nu}$ for different systems sizes should collapse into one for the appropriate value of ν. This technique is known as full data collapsing and the results of such approach are shown in Fig. 5. As it can be seen in this figure, a very good collapse of the different curves is obtained, using the exact value of the critical exponent for the two-dimensional $q - 3$ Potts universality class, $\nu = 5/6$.

The remaining scaling behavior associated with the critical exponents, β and γ, can be obtained from the data collapsing curves of the order parameter δ and susceptibility χ according to Eqs. (8) and (9), respectively. In Fig. 6, $\delta L^{\beta/\nu}$ is plotted as a function of $|\epsilon|L^{1/\nu}$ (log scale in both axes) and a very good result can be seen for the value $\beta = 1/9$, which, again, is the exact exponent for the two-dimensional $q - 3$ Potts universality class. Finally, in Fig. 7, the collapsing of the curves of $\chi L^{-\gamma/\nu}$ vs $\epsilon L^{1/\nu}$ for triangular lattices of different sizes is shown and an excellent fit is produced for $\gamma = 13/9$, once again matching the exact value of the exponent for the two-dimensional $q - 3$ Potts universality class.

A complementary analysis can be made by estimating the critical coverage by a different methodology. FSS theory provides several routes to estimate critical quantities from MC simulations [46–48,59]. An alternative method to the crossing of the cumulants (Fig. 4) consists in estimating θ_c from the

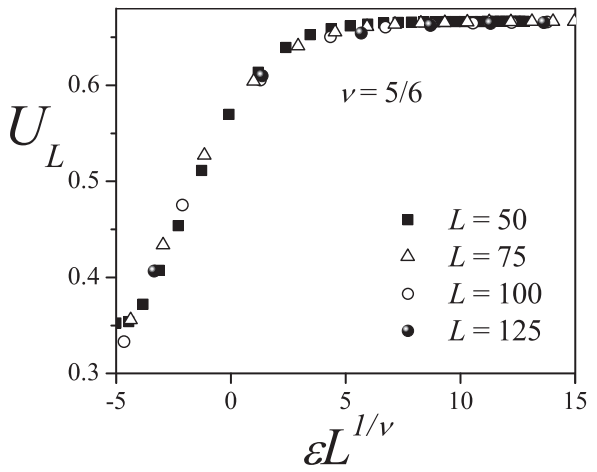

FIG. 5. Full data collapsing of the cumulants, U_L vs $\varepsilon L^{1/\nu}$ for different sizes: $L = 50$, solid squares; $L = 75$, open triangles; $L = 100$, open circles; and $L = 125$, spheres. The plots were made using $\theta_c = 0.792$ and $\nu = 5/6$.

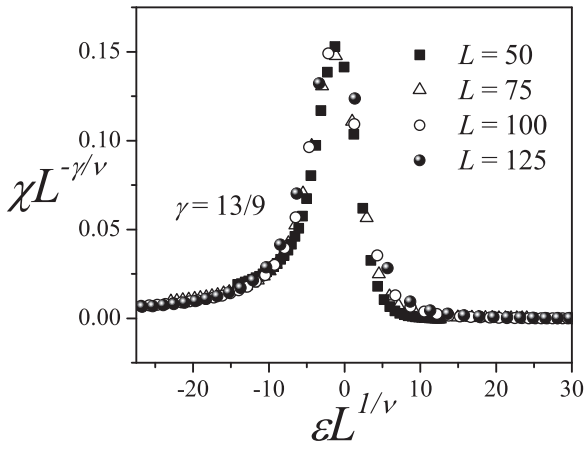

FIG. 7. Data collapsing of the susceptibility χ for different sizes: $L = 50$, solid squares; $L = 75$, open triangles; $L = 100$, open circles; and $L = 125$, spheres. The collapse is produced for $\theta_c = 0.792$, $\nu = 5/6$, $\beta = 1/9$, and $\chi = 13/9$.

extrapolation of the location $\theta_c(L)$ of the maxima of several different thermodynamic quantities. This method relies in the fact that the locations of these maxima $\theta_c(L)$ exhibit an scaling behavior with system size according to

$$\theta_c(L) = \theta_c(\infty) + AL^{1/\nu}, \tag{11}$$

where A is a constant that depends on the thermodynamic quantity considered. In Fig. 8 we show a plot of $\theta_c(L)$ vs $L^{1/\nu}$ for the maximum values of three classical FSS quantities such as the susceptibility $\chi(\theta)$, and the logarithmic derivatives of $\delta(\theta)$ and $\delta^2(\theta)$, along with the maxima of the mutability $\zeta_\delta(\theta)$ and diversity $D_\delta(\theta)$ of the order parameter, two nontraditional FSS quantities that belong to the information theory.

The high degree of compression recognized by WLZIP means that specific repetitive information has been detected along the data chain; this is characteristic of a monotonic behavior, suggesting that the system does not alter its properties within the data window under consideration. On the other hand, near a critical point, where a chaotic succession of data should occur, WLZIP will compress very little, giving higher values for mutability and diversity. Thus, what WLZIP should give is high contrast between monotonic regimes as compared to chaotic regimes. Consequently, a maximum is observed in the curve of $\zeta_\delta(\theta)$ [$D_\delta(\theta)$] as a function of the coverage. The positions of these maxima are collected in Fig. 8: open circles (mutability) and spheres (diversity). The different lattice sizes used in the simulations are indicated in the figure. The dashed lines represent linear fits of the data according to Eq. (11) with $\nu = 5/6$. An estimate of the critical coverage is

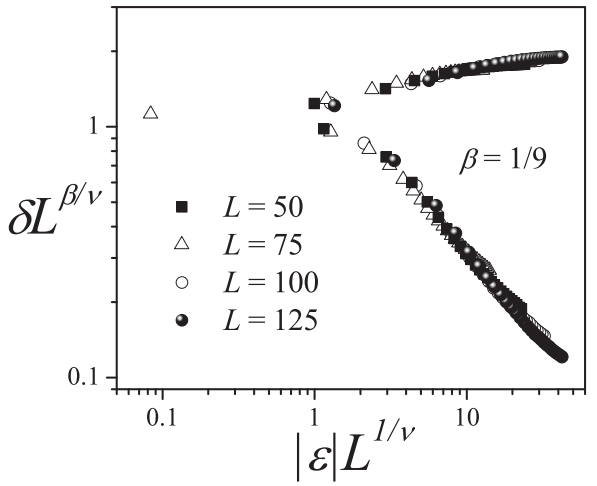

FIG. 6. Data collapsing of the nematic order parameter δ in logarithmic scale for different sizes: $L = 50$, solid squares; $L = 75$, open triangles; $L = 100$, open circles; and $L = 125$, spheres. The collapse is produced for $\theta_c = 0.792$, $\nu = 5/6$, and $\beta = 1/9$.

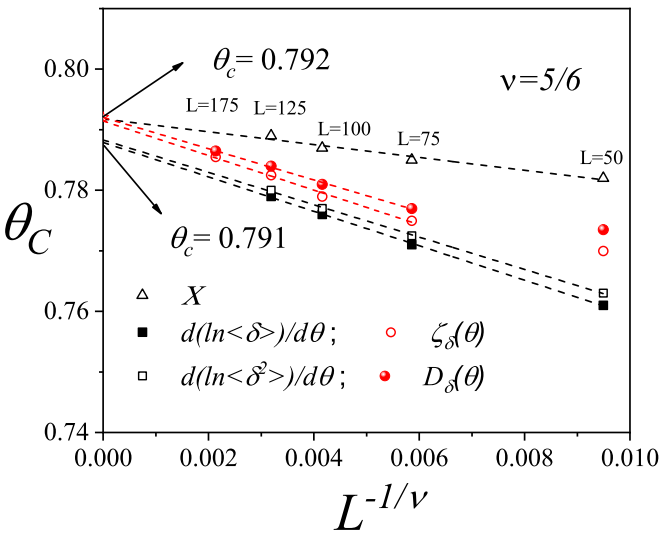

FIG. 8. Location of the maximum value θ_c vs $L^{1/\nu}$ from several quantities, susceptibility χ, the logarithmic derivatives of δ and δ^2, the mutability ζ_δ, and the diversity D_δ of the order parameter. Dashed lines correspond to linear fits of the data. The data corresponding to $L = 50$ were excluded from the fits of the mutability and diversity. From extrapolation one obtains the critical coverage at the thermodynamic limit $\theta_c(L = \infty)$.

obtained from extrapolation toward the thermodynamic limit $L = \infty$. As it can be seen, the estimated θ_c from the the logarithmic derivatives of $\delta(\theta)$ and $\delta^2(\theta)$ deviates a little from the value predicted by the Binder cumulants (Fig. 4). On the other hand, the estimates provided by the extrapolation of the susceptibility data, and, surprisingly, also from the indicators of the information theory, yields very close estimates in very good agreement with the critical coverage obtained from the crossing of the cumulants. Strong deviation from the scaling behavior of the mutability and diversity were found for the $L = 50$ system and therefore those points were excluded from the fits, and an extra value was calculated for a larger system of size $L = 175$.

IV. SUMMARY AND CONCLUSIONS

In this work, we have used Monte Carlo simulations and finite-size scaling theory to resolve the nature and universality class of the IN phase transition occurring in a model of self-assembled 2-thiophene molecules adsorbed on Au(111) surfaces, modelled as rigid multipolar pentamers adsorbed on a 2D rhombus-shaped triangular lattice.

Based on previous density functional theory calculations, we defined three equivalent lying directions for the adsorption of any molecule over the substrate. Accordingly, the gold surface was discretized and modeled as a 2D $L \times L$ triangular lattice. On the other hand, the 2-thiophene molecules were modeled as rigid linear k-mers, with $k = 5$ or pentamers. In order to capture the multipolar essence of these molecules and their nonhomogeneous intermolecular interactions, three different interaction centers along the pentamers were defined, both ends (heads) and the center element of the chain. The remaining two intermediate elements of the chain were considered neutral. Therefore, three different interaction energies were defined: head-head (w_{HH}), head-center (w_{HC}), and center-center (w_{CC}). Interaction energies and the relationships between them, expressed in k_BT units, were $w_{\mathrm{HH}} = 1.0$, $w_{\mathrm{HC}} = 0.5w_{\mathrm{HH}} = 0.5$, and $w_{\mathrm{CC}} = 1.5w_{\mathrm{HH}} = 1.5$. Under these considerations, the resulting lattice-gas model reproduces very well the interaction energies measured by Flores *et al.* [42] using DFT calculations.

A nematic phase, characterized by a big domain of parallel molecules, was found. This ordered phase is separated from the isotropic state by a continuous transition occurring at an intermediate density $\theta_c = 0.792(1)$. Such phase transition indicates that this may be a mechanism for the 2-thiophene molecules to form a self-assembled monolayer over the Au(111) surface in agreement with previously reported experimental results [42].

The behavior of the present model contrasts with that observed for the case of straight rigids rods with homogeneous (or zero) lateral interactions, where the IN phase transition occurs for k-mer sizes $k \geqslant 7$ [17,18]. Our results here are important from a theoretical point of view, complement those obtained for the noninteracting problem, and could have potential application in the field of self-assembled monolayers on metallic substrates. Experimental studies in these systems have shown that their electronic and transport properties can be adjusted by tuning the competition between the molecule-substrate and intermolecular interactions. The findings obtained in this work provide an important contribution in this direction, demonstrating that the inclusion of different interaction centers in the adsorbate strongly determines the possible structures that appear on the surface with increasing density. Thus, our theoretical predictions can guide future experiments investigating the adsorption of multipolar molecules. These systems, apparently governed by the structure of the molecule and intermolecular interactions, have promissory technological applications.

The critical exponents were accurately determined from finite-size scaling analysis, being $\nu = 0.835(5)$, $\beta = 0.118(6)$, and $\gamma = 1.453(6)$. The obtained values of ν, β, and γ clearly indicate that the observed IN phase transition belongs to the universality class of the two-dimensional Potts model [60] with $q = 3$. This finding is consistent with the three competing ordered states near the transition. In the nematic phase, the adsorbed molecules spontaneously align over one of the three allowed directions of the lattice.

In addition to conventional quantities, the finite-size scaling analysis also included the study of mutability and diversity. These two quantities are derived from dynamical information theory and are not part of the conventional treatment of the thermodynamic phase transitions. It is shown that the critical exponent ν can be obtained from the scaling behavior of the diversity. In addition, the estimates of the critical coverage provided by the extrapolation of the maxima of mutability and diversity are in excellent agreement with the corresponding ones obtained from the conventional scaling quantities (order parameter and its derivatives and susceptibility). To the authors knowledge, this is the first time that it is shown that quantities from information theory can be employed in FSS analyses. The findings obtained here contribute to the understanding of critical phenomena from novel compression algorithms for studying mutual information in sequences of data.

Future efforts will be done following two directions: first, to extend the methodology exposed in this work (MC simulations, information theory, and finite-size scaling) to understand and/or follow surface phase transitions for other kind of molecules deposited over different substrates and, second, to study the effect of nonhomogeneous lateral interactions on the minimum value of k, which allows the formation of the nematic phase in a model of interacting straight rigid k-mers adsorbed on two-dimensional substrates.

ACKNOWLEDGMENTS

This work was supported in part by CONICET (Argentina) under Project No. PIP 112-201101-00615 and Universidad Nacional de San Luis (Argentina) under Project No. 03-1920. The numerical works were done using the BACO parallel cluster [61] located at Instituto de Física Aplicada, Universidad Nacional de San Luis-CONICET, San Luis, Argentina. In addition partial support is also acknowledged from Center for Nanoscience and Nanotechnology CEDENNA (ANID Contract No. 1180001, Chile) and Fondecyt (Contract No. 1190036, Chile).

[1] S. Casalini, C. A. Bortolotti, F. Leonardi, and F. Biscarini, Self-assembled monolayers in organic electronics, Chem. Soc. Rev. **46**, 40 (2017).

[2] Y. Zhou, M. Su, X. Yu, Y. Zhang, J.-G. Wang, X. Ren, R. Cao, W. Xu, D. R. Baer, Y. Du *et al.*, Real-time mass spectrometric characterization of the solid–electrolyte interphase of a lithium-ion battery, Nat. Nanotechnol. **15**, 224 (2020).

[3] X. Zhang, C. Gong, O. U. Akakuru, Z. Su, A. Wu, and G. Wei, The design and biomedical applications of self-assembled two-dimensional organic biomaterials, Chem. Soc. Rev. **48**, 5564 (2019).

[4] Z. Zhang and S. C. Glotzer, Self-assembly of patchy particles, Nano Lett. **4**, 1407 (2004).

[5] C. A. Palma, M. Cecchini, and P. Samorì, Predicting self-assembly: From empirism to determinism, Chem. Soc. Rev. **41**, 3713 (2012).

[6] A. Ghosh, E. T. Dobson, C. J. Buettner, M. J. Nicholl, and J. E. Goldberger, Programming ph-triggered self-assembly transitions via isomerization of peptide sequence, Langmuir **30**, 15383 (2014).

[7] C. Buettner, A. Wallace, S. Ok, A. Manos, M. Nicholl, A. Ghosh, M. Tweedle, and J. Goldberger, Balancing the intermolecular forces in peptide amphiphiles for controlling self-assembly transitions, Org. Biomolec. Chem. **15**, 5220 (2017).

[8] L. Onsager, The effects of shape on the interaction of colloidal particles, Ann. N. Y. Acad. Sci. **51**, 627 (1949).

[9] J. Straley, Liquid crystals in two dimensions, Phys. Rev. A **4**, 675 (1971).

[10] D. Frenkel and R. Eppenga, Evidence for algebraic orientational order in a two-dimensional hard-core nematic, Phys. Rev. A **31**, 1776 (1985).

[11] A. Ghosh and D. Dhar, On the orientational ordering of long rods on a lattice, Europhys. Lett. **78**, 20003 (2007).

[12] M. Disertori and A. Giuliani, The nematic phase of a system of long hard rods, Commun. Math. Phys. **323**, 143 (2013).

[13] D. Dhar, R. Rajesh, and J. F. Stilck, Hard rigid rods on a bethe-like lattice, Phys. Rev. E **84**, 011140 (2011).

[14] D. Matoz-Fernandez, D. Linares, and A. Ramirez-Pastor, Determination of the critical exponents for the isotropic-nematic phase transition in a system of long rods on two-dimensional lattices: Universality of the transition, Europhys. Lett. **82**, 50007 (2008).

[15] D. A. Matoz-Fernandez, D. H. Linares, and A. J. Ramirez-Pastor, Critical behavior of long linear k-mers on honeycomb lattices, Physica A **387**, 6513 (2008).

[16] D. Matoz-Fernandez, D. Linares, and A. Ramirez-Pastor, Critical behavior of long straight rigid rods on two-dimensional lattices: Theory and monte carlo simulations, J. Chem. Phys. **128**, 214902 (2008).

[17] P. Longone, D. Linares, and A. Ramirez-Pastor, Critical behavior of attractive rigid rods on two-dimensional lattices, J. Chem. Phys. **132**, 184701 (2010).

[18] P. Longone, M. Dávila, and A. J. Ramirez-Pastor, Isotropic-nematic phase diagram for interacting rigid rods on two-dimensional lattices, Phys. Rev. E **85**, 011136 (2012).

[19] T. Fischer and R. Vink, Restricted orientation "liquid crystal" in two dimensions: Isotropic-nematic transition or liquid-gas one (?), Europhys. Lett. **85**, 56003 (2009).

[20] J. Kundu and R. Rajesh, Asymptotic behavior of the isotropic-nematic and nematic-columnar phase boundaries for the system of hard rectangles on a square lattice, Phys. Rev. E **91**, 012105 (2015).

[21] D. Linares, F. Romá, and A. Ramirez-Pastor, Entropy-driven phase transition in a system of long rods on a square lattice, J. Stat. Mech.: Theory Exp. (2008) P03013.

[22] J. Kundu, R. Rajesh, D. Dhar, and J. F. Stilck, A Monte Carlo algorithm for studying phase transition in systems of hard rigid rods, in *Solid State Physics:Proceedings of the 56th DAE Solid State Physics Symposium 2011*, edited by R. Mittal, A. K. Chauhan, and R. Mukhopadhyay, AIP Conf. Proc. No. 1447 (American Institute of Physics, Melville, NY, 2012), pp. 113–114.

[23] J. Kundu, R. Rajesh, D. Dhar, and J. F. Stilck, Nematic-disordered phase transition in systems of long rigid rods on two-dimensional lattices, Phys. Rev. E **87**, 032103 (2013).

[24] E. E. Vogel, G. Saravia, and A. J. Ramirez-Pastor, Phase transitions in a system of long rods on two-dimensional lattices by means of information theory, Phys. Rev. E **96**, 062133 (2017).

[25] E. E. Vogel, G. Saravia, A. J. Ramirez-Pastor, and M. Pasinetti, Alternative characterization of the nematic transition in deposition of rods on two-dimensional lattices, Phys. Rev. E **101**, 022104 (2020).

[26] E. Vogel, G. Saravia, F. Bachmann, B. Fierro, and J. Fischer, Phase transitions in Edwards–Anderson model by means of information theory, Physica A **388**, 4075 (2009).

[27] E. Vogel, G. Saravia, and L. Cortez, Data compressor designed to improve recognition of magnetic phases, Physica A **391**, 1591 (2012).

[28] V. Cortez, G. Saravia, and E. Vogel, Phase diagram and reentrance for the 3d Edwards–Anderson model using information theory, J. Magn. Magn. Mater. **372**, 173 (2014).

[29] D. Dhar and R. Rajesh, Entropy of fully packed hard rigid rods on d-dimensional hypercubic lattices, Phys. Rev. E **103**, 042130 (2021).

[30] P. M. Pasinetti, A. J. Ramirez-Pastor, E. E. Vogel, and G. Saravia, Entropy-driven phases at high coverage adsorption of straight rigid rods on two-dimensional square lattices, Phys. Rev. E **104**, 054136 (2021).

[31] A. Shah, D. Dhar, and R. Rajesh, Phase transition from nematic to high-density disordered phase in a system of hard rods on a lattice, Phys. Rev. E **105**, 034103 (2022).

[32] J. M. Tavares, B. Holder, and M. M. Telo da Gama, Structure and phase diagram of self-assembled rigid rods: Equilibrium polydispersity and nematic ordering in two dimensions, Phys. Rev. E **79**, 021505 (2009).

[33] R. Zwanzig, First-order phase transition in a gas of long thin rods, J. Chem. Phys. **39**, 1714 (1963).

[34] L. G. López, D. H. Linares, and A. J. Ramirez-Pastor, Critical exponents and universality for the isotropic-nematic phase transition in a system of self-assembled rigid rods on a lattice, Phys. Rev. E **80**, 040105(R) (2009).

[35] N. G. Almarza, J. M. Tavares, and M. M. Telo da Gama, Effect of polydispersity on the ordering transition of adsorbed self-assembled rigid rods, Phys. Rev. E **82**, 061117 (2010).

[36] L. López, D. Linares, A. Ramirez-Pastor, and S. Cannas, Phase diagram of self-assembled rigid rods on two-dimensional lattices: Theory and Monte Carlo simulations, J. Chem. Phys. **133**, 134706 (2010).

[37] L. López, D. Linares, and A. Ramirez-Pastor, Critical behavior of self-assembled rigid rods on triangular and honeycomb lattices, J. Chem. Phys. **133**, 134702 (2010).
[38] N. G. Almarza, J. Tavares, and M. T. da Gama, Communication: The criticality of self-assembled rigid rods on triangular lattices, J. Chem. Phys. **134**, 071101 (2011).
[39] L. G. López, D. H. Linares, and A. J. Ramirez-Pastor, Comment on "effect of polydispersity on the ordering transition of adsorbed self-assembled rigid rods," Phys. Rev. E **85**, 053101 (2012).
[40] N. G. Almarza, J. M. Tavares, and M. M. Telo da Gama, Reply to "comment on effect of polydispersity on the ordering transition of adsorbed self-assembled rigid rods," Phys. Rev. E **85**, 053102 (2012).
[41] E. Cisternas, G. dos Santos, M. Flores, E. E. Vogel, and A. J. Ramirez-Pastor, Self-assembled monolayer formation of pentamers-like molecules onto FCC(111) surfaces: The case of curcuminoids onto Au (111) surface, Nano Expr. **1**, 010025 (2020).
[42] M. Flores, E. Cisternas, A. Mella, D. Jullian, A. Nunez, and M. Soler, Adsorption of 2-thiophene curcuminoid molecules on a Au (111) surface, Appl. Surf. Sci. **427**, 620 (2018).
[43] J. Jia, A. Giglia, M. Flores, O. Grizzi, L. Pasquali, and V. A. Esaulov, 1, 4-benzenedimethanethiol interaction with Au(110), Ag(111), Cu(100), and Cu(111) surfaces: self-assembly and dissociation processes, J. Phys. Chem. C **118**, 26866 (2014).
[44] E. H. Lieb, Exactly soluble models, Physica **73**, 226 (1974).
[45] M. E. Fisher, in *Critical Phenomena*, 1st ed., edited by M. S. Green (Academic Press, London, 1971).
[46] K. Binder, *Applications of the Monte Carlo Method in Statistical Physics: Topics in Current Physics* (Springer, Berlin, 1984).
[47] V. Privman, *Finite Size Scaling and Numerical Simulation of Statistical Systems* (World Scientific, Singapore, 1990).
[48] V. Privman, P. C. Hohenberg, and A. Aharony, in *Phase Transitions and Critical Phenomena*, edited by C. Domb and J. L. Lebowitz, Vol. 14 (Academic, New York, 1991).
[49] H. Müller-Krumbhaar and K. Binder, *Monte Carlo Methods in Statistical Physics, Topics in Current Physics* (Springer-Verlag, Berlin, 1979).
[50] R. Avinery, M. Kornreich, and R. Beck, Universal and Accessible Entropy Estimation Using a Compression Algorithm, Phys. Rev. Lett. **123**, 178102 (2019).
[51] E. E. Vogel and G. Saravia, Information theory applied to econophysics: Stock market behaviors, Eur. Phys. J. B **87**, 1 (2014).
[52] E. Vogel, G. Saravia, J. Astete, J. Díaz, and F. Riadi, Information theory as a tool to improve individual pensions: The Chilean case, Physica A **424**, 372 (2015).
[53] D. J. Contreras, E. E. Vogel, G. Saravia, and B. Stockins, Derivation of a measure of systolic blood pressure mutability: A novel information theory-based metric from ambulatory blood pressure tests, J. Am. Soc. Hypertens. **10**, 217 (2016).
[54] E. Vogel, G. Saravia, D. Pasten, and V. Munoz, Time-series analysis of earthquake sequences by means of information recognizer, Tectonophysics **712-713**, 723 (2017).
[55] N. Metropolis, A. W. Rosenbluth, M. N. Rosenbluth, A. H. Teller, and E. Teller, Equation of state calculations by fast computing machines, J. Chem. Phys. **21**, 1087 (1953).
[56] R. H. Swendsen and J.-S. Wang, Replica Monte Carlo Simulation of Spin-Glasses, Phys. Rev. Lett. **57**, 2607 (1986).
[57] D. J. Earl and M. W. Deem, Parallel tempering: Theory, applications, and new perspectives, Phys. Chem. Chem. Phys. **7**, 3910 (2005).
[58] K. Hukushima and K. Nemoto, Exchange Monte Carlo method and application to spin glass simulations, J. Phys. Soc. Jpn. **65**, 1604 (1996).
[59] A. M. Ferrenberg and D. P. Landau, Critical behavior of the three-dimensional Ising model: A high-resolution Monte Carlo study, Phys. Rev. B **44**, 5081 (1991).
[60] F.-Y. Wu, The Potts model, Rev. Mod. Phys. **54**, 235 (1982).
[61] Available at http://cluster_infap.unsl.edu.ar/wordpress.